Space-time double correlations and spectra in a turbulent boundary layer

By A. J. FAVRE, J. J. GAVIGLIO, and R. DUMAS
Laboratoire de Mécanique de l'Atmosphère, Université de Marseille

(*Received* 3 *September* 1956 *and in revised form* 30 *January* 1957)

SUMMARY

This paper describes the results of an experimental investigation of the turbulent boundary layer on a flat plate with zero pressure gradient, carried out at the Laboratoire de Mécanique de l'Atmosphère (I.M.F. Marseille). Transition to turbulent flow was obtained either by increasing the preturbulence upstream of the plate by means of a grid, or by a series of emery paper roughness elements beginning at the leading edge. The measurements were of the space-time double correlations, i.e. double velocity correlations with both spatial separation and time delay, from which isocorrelation lines for optimum delay can be drawn, and of the spectrum function, all for the longitudinal component of the velocity fluctuation.

1. EXPERIMENTAL APPLIANCES

Most of these have been described in previous papers (Favre, Gaviglio & Dumas, 1952, 1953 b, 1954 a, 1954 b).

The wind-tunnel has a complete return circuit, and is operated by two contra-rotating fans whose pitch is adjustable during operation. The fans are driven by two direct-current motors, fed by a 60 H.P. regulated ignitron rectifier, making it possible to change the rotation speed. The test section is 80 cm × 80 cm × 270 cm. There is a smooth contraction with an area ratio of 15; it is preceded by a settling chamber, in which five damping screens are set, and by a rapid expansion diffuser, with a screen analogous to that of the low-turbulence wind-tunnel of the R.A.E. (Squire, Winter & Barnes 1947). The natural intensity ratio of the turbulence in the test section is 0·00038 for a speed of 12·20 m/sec.

A flat plate made of glass (Favre, Gaviglio & Dumas 1954 a), 210 cm in length and 80 cm in width, and with a profiled leading edge, was hung in the test section. The measurements have been made, as previously, under the lower side of the plate at distances from the leading edge of about 80 cm and 194 cm.

y' and y are distances from the walls of the wires A (fixed) and B (adjustable); $X_3 = y' - y$ (figure 1); $CB = X_1$ is their separation in the direction of the general stream velocity; their separation X_2 parallel to the plate and normal to the stream is zero. T is the interval of time added to the instant of the signal corresponding to the fixed wire A.

The hot-wire probes used were either of an old pattern (diameter of the body 10 mm—see figure 1) or of a new type (diameter of the body 8 mm, with holders thinned and lengthened); the holders of the upstream probe were made lozenge-shaped in order to lessen the effects of the wake.

The platinum hot wire was made by the wollaston process with an etched length 7 μ in diameter and about 1 mm in length. In the position $z = 194$ cm, the new type of probe holder was used. This holder, fixed to the upper side of the plate, passed round the trailing edge and was supported on the lower side. It allowed variation of X_1, X_2, X_3.

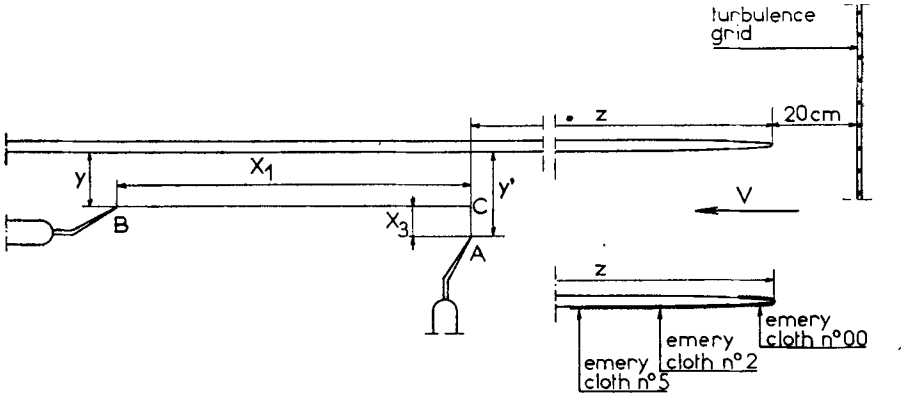

Figure 1. Experimental arrangement: transition by roughness on leading edge, or by preturbulence downstream of a grid.

Transition to turbulent flow in the boundary layer was obtained either by increasing the preturbulence of the stream by means of a biplane grid of mesh $M = 1$ in. with rods of circular section ($d = 0{\cdot}5$ cm) (Favre, Gaviglio & Dumas 1952) set at 20 cm upstream of the leading edge of the plate (figure 1), or by inserting, starting at this leading edge (figure 1), roughness in the form of emery cloth (no. 00 up to $z = 20$ cm, then no. 2 to $z = 30$ cm, and then no. 5 to $z = 40$ cm).

The principal measuring appliances were the hot-wire anemometers reproducing the oscillations, within $\pm 4\%$ in energy from 1 to 3500 hertz, the spectral analyser with a selectivity of 4·5% of the median frequency and a measuring band extending from 1 to 5000 hertz, and the apparatus for measurement of time and space correlations (Favre 1946, 1948; Favre, Gaviglio & Dumas 1953 a) with a band-pass extending from 1 to 2500 hertz. This latter apparatus records simultaneously, and reproduces with a relative delay, the two voltages coming from the two anemometers, and measures the time-correlation coefficient.

2. Checks on the measurements

We tried to check the influence of the disturbances due to the upstream wire (platinum wire, silver coating, needles, body of the probe) on the precision of measurements of the intensities of turbulence, the local mean

velocity and the space-time correlation (Favre, Gaviglio & Dumas 1955). With the old type of probes the disturbances in unfavourable conditions (upstream wire near the wall) may have reached 10% of the turbulence intensities, 5% of the mean velocity, and 0·05% of the space-time correlation. With the new type probes these disturbances seemed to be reduced to 4% for intensities and to 1% for the mean velocity.

We have verified, thanks to a method proposed by H. W. Liepmann (1952), that the length of the hot wires had a negligible influence on the measurements of space-time correlation (for these experimental investigations, the minimum value of the dissipation length λ was 2·5 mm).

3. Mean velocities

The velocity V_{max} outside the boundary layer was 12·00 m/sec. In the case of the measurements made at $x = 79$ cm, with hot-wire holders, the mean gradient of static pressure is negative and less than 4% per metre. For the measurements made at $x = 194$ cm, with the new holders, the mean gradient is negative and less than 1% per metre downstream of the roughness.

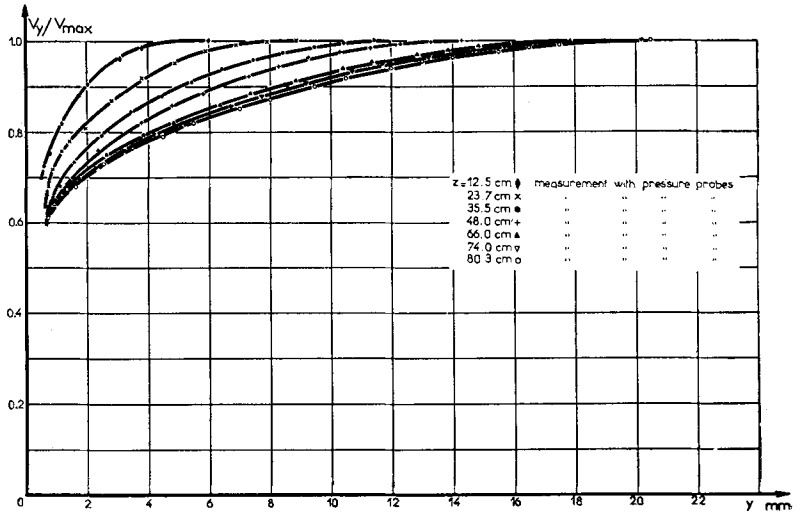

Figure 2. Mean velocity in the boundary layer on a flat plate downstream of a grid.

In the case of the boundary layer on a flat plate downstream of a turbulence grid, the relative velocities V_y/V_{max} were determined as a function of the distance y from the wall, for $x = 12{\cdot}5$, 23·7, 35·5, 48·0, 66·0, 74·0, 80·3 cm, and the results are shown in figure 2. The thickness of the boundary layer at 79 cm from the leading edge was 16·8 mm.

In the case of the boundary layer on a flat plate with a rough leading edge, the velocity profiles were measured, in the absence of the hot-wire holders, at $x = 58{\cdot}5$, 79·0, 167·5 and 194·0 cm, and are given in figure 3. A supplementary curve has been drawn to show the effect of the presence

of the holders. The velocity V_y in the vicinity of the wall was determined at $x = 194$ cm by means of a hot wire. The thickness of boundary layer in this case was 17·5 mm at $x = 79$ cm, and 34 mm at $x = 194$ cm.

In figure 4 we have represented the displacement thickness δ^* and the momentum thickness θ as functions of the distance x from the leading edge. The roughness set on the leading edge brings about a marked increase in the thickness of the boundary layer.

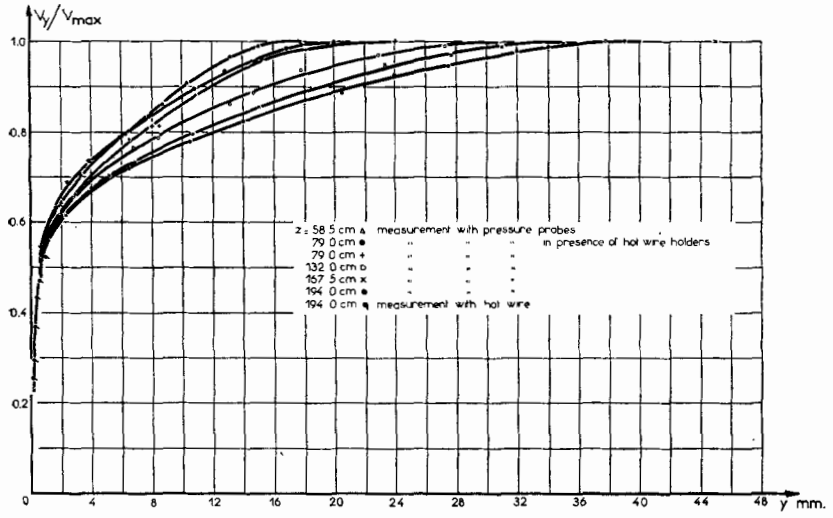

Figure 3. Mean velocity in the boundary layer on a flat plate with a rough leading edge.

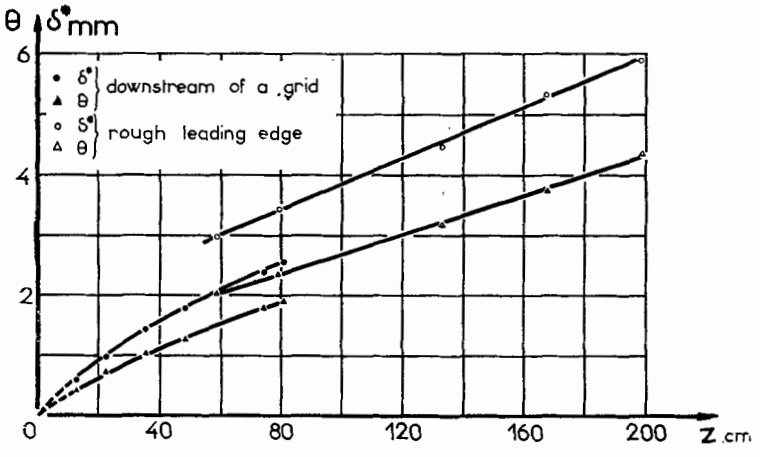

Figure 4. Displacement thickness δ^* and momentum thickness θ.

Figure 5 shows Clauser's universal velocity profile (Clauser 1954). In this figure, $V_* = \sqrt{(\tau_0/\rho)}$ with $\tau_0 = \rho V_{\max}^2 \, d\theta/dx$, and the value of δ corresponds to $V_y/V_{\max} \doteq 1$. In the case of transition obtained by preturbulence (in the presence of the old type of wire holders, the mean

pressure gradient being 4% per metre) the data are not wholly consistent with the curve, but in the case of transition obtained by roughness (with the new type of holders, the mean pressure gradient being 1% per metre) the agreement between the data and the curve is fairly good.

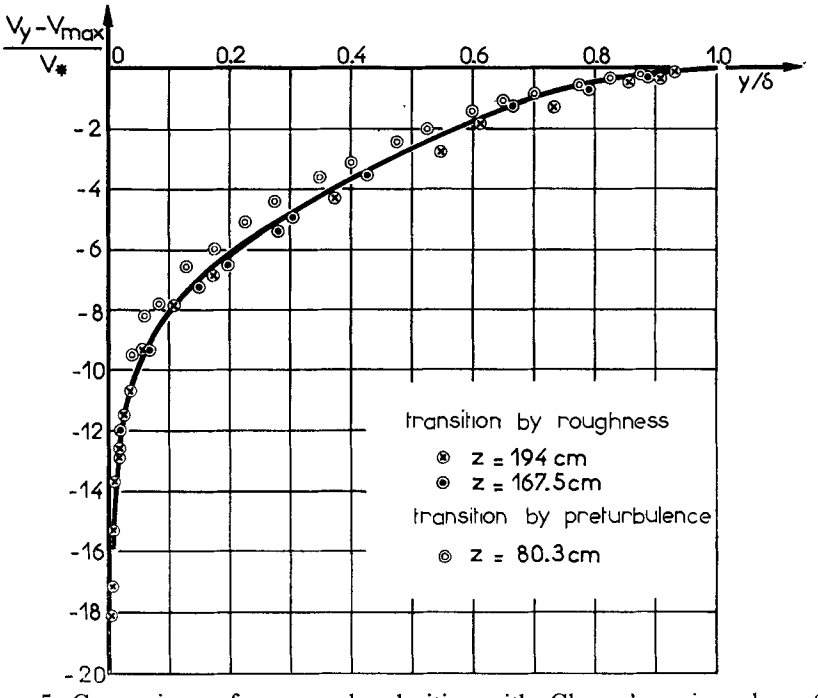

Figure 5. Comparison of measured velocities with Clauser's universal profile.

4. Intensities and spectra

In the case of transition by preturbulence, the intensities as functions of the distance y/δ have been given previously (Favre, Gaviglio & Dumas 1954a). The intensity $\sqrt{(\overline{v_1^2})}/V_y$ reaches 15% for $y/\delta = 0{\cdot}06$, which may be compared with the value 1·8% for the intensity of free turbulence at a great distance from the wall. In the case of the transition by roughness, two series of measurements have been made, at $z = 79$ cm and $z = 194$ cm. The intensity, as a fraction of the local mean velocity, seems to decrease more rapidly at $z = 194$ cm than at $z = 79$ cm when y/δ increases. At $z = 79$ cm, it reaches 18% for $y/\delta = 0{\cdot}06$, that of the free turbulence being of the order of 0·045%.

The spectral functions of turbulence energy $F(n)$ (Taylor 1938) are obtained as functions of the frequency n; directly by selective amplification, and indirectly by Fourier transformation of the auto correlation curves.

The areas of the curves $F(n)$ have been chosen so as to be equal for the common intervals of frequencies.

In the case of transition by preturbulence, the spectra have been published previously (Favre, Gaviglio & Dumas 1954a). They correspond

to $z = 79$ cm. The difference between these spectra inside and outside the boundary layer is small, except for low frequencies (less than 40 hertz) where they change markedly as functions of the distance from the wall, thus disclosing an increase of energy in the boundary layer.

In the case of transition by roughness, unlike the previous case, the intensity of turbulence is very low outside the boundary layer (0·045%). Figure 6 shows the spectra measured at 79 cm from the leading edge for

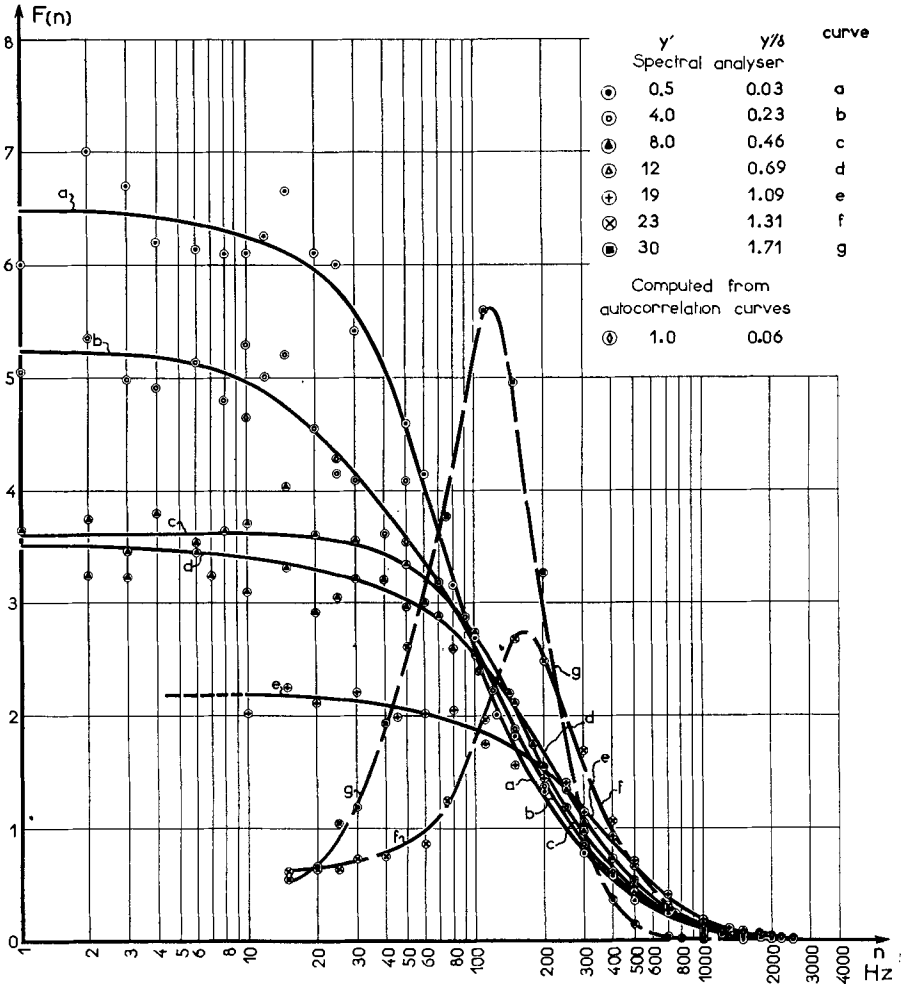

Figure 6. Turbulence spectra in the boundary layer on a flat plate with rough leading edge. ($R_\delta = 14\,500$, $z = 79$ cm).

different distances y from the plate. Inside the boundary layer the evolution at frequencies greater than 80 hertz is slight; for the lower frequencies the curves show an increase of energy as y/δ decreases. Outside the conventional boundary layer, at $y/\delta = 1{\cdot}31$ and $y/\delta = 1{\cdot}71$ (the factor of intermittance there being markedly smaller than 0·04 according to

Corrsin & Kistler (1954)), the spectra become different; each of them presents a marked maximum. At the distance $z = 194$ cm from the leading edge (figure 7) the results are qualitatively the same, but with lower frequencies, which corresponds to the increase of the scale of turbulence with the thickness of the boundary layer. Outside the boundary layer, for instance, at $y/\delta = 1{\cdot}35$ and $y/\delta = 1{\cdot}77$, a marked maximum was found as in the previous case.

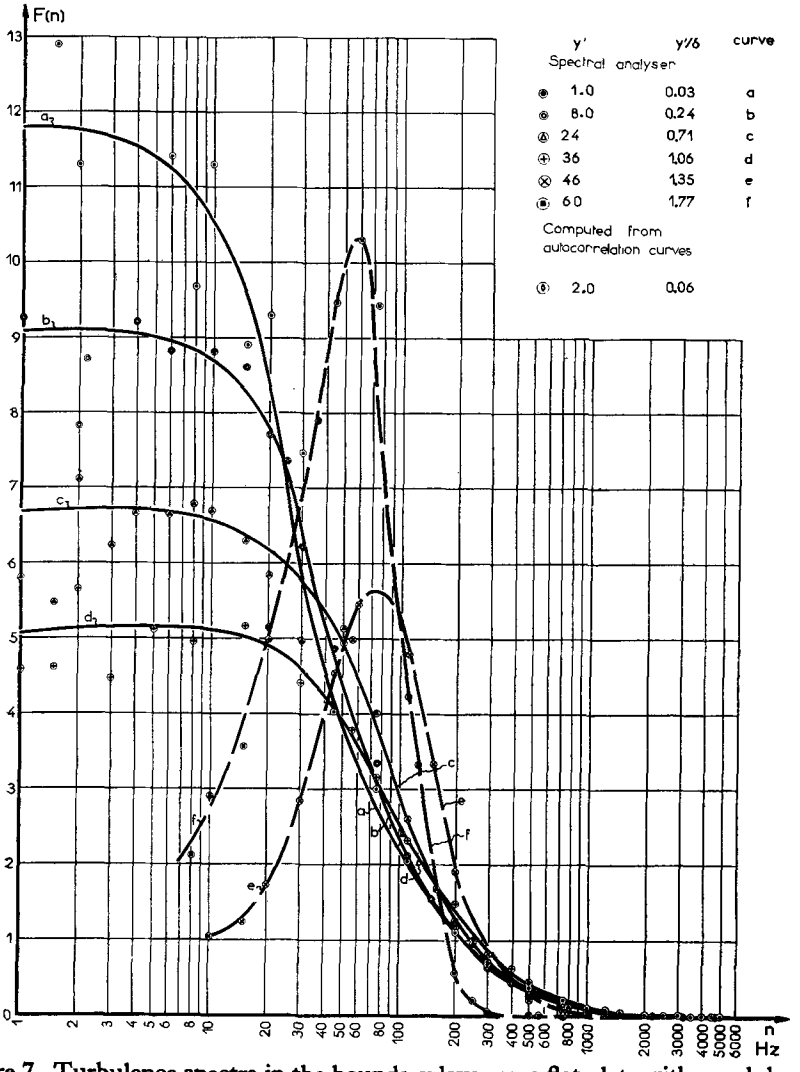

Figure 7. Turbulence spectra in the boundary layer on a flat plate with rough leading edge. ($R_\delta = 28\,000$, $z = 194$ cm).

The intensities of these fluctuations outside the boundary layer are 0·47% and 0·17% respectively for $y/\delta = 1{\cdot}31$ and 1·71 ($z = 79$ cm), and 0·38% and 0·13% for $y/\delta = 1{\cdot}35$ and 1·77 ($z = 194$ cm). Thus, they do not seem to be due to the preturbulence, the intensity of which is of 0·045%.

When we inserted a small thin plate (4·2 cm × 12·5 cm) parallel to the wall, at $y/\delta = 1{\cdot}25$, between the hot wire placed at $y/\delta = 1{\cdot}8$ ($z = 79$ cm) and this wall, the intensity was reduced by more than half and this phenomenon was no longer detected.

It may be that these fluctuations are induced by random motion at the edge of the boundary layer (Phillips 1954).

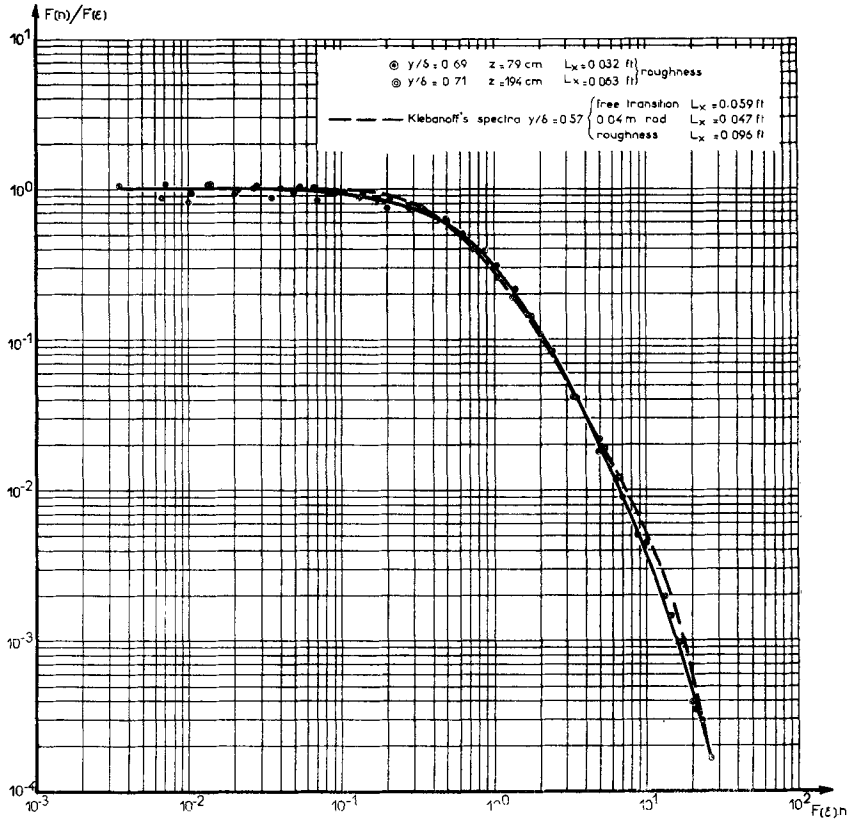

Figure 8. Comparison of turbulence spectra in several boundary layers on flat plates.

We have compared (figure 8) the spectra obtained for $z = 79$ cm and $z = 194$ cm (y/δ having respectively the neighbouring values 0·69 and 0·71), with Klebanoff & Diehl's (1952) spectra. The ordinates and abscissae in figure 8 are $F(n)/F(\epsilon)$ and $nF(\epsilon)$, $F(\epsilon)$ being the average value corresponding to the lowest frequencies. The results are fairly consistent.

5. Measurements of space-time correlations

First consider the measurements of transverse space-time correlations $R_{11}(T, X_1 = 0, X_2 = 0, X_3)$.

In the case of transition by preturbulence, the transverse space-time correlation $R_{11}(T, X_1 = 0, X_2 = 0, X_3)$ is represented in figures 9 to 12.

The data for these figures are:

figure 9,	$y'/\delta = 0{\cdot}06$,	$y' = 1$ mm,	$z = 79$ cm;
figure 10,	$y'/\delta = 0{\cdot}06$,	$y' = 1$ mm,	$z = 74$ cm;
figure 11,	$y'/\delta = 0{\cdot}24$,	$y' = 4$ mm,	$z = 79$ cm;
figure 12,	$y'/\delta = 0{\cdot}71$,	$y' = 12$ mm,	$z = 79$ cm.

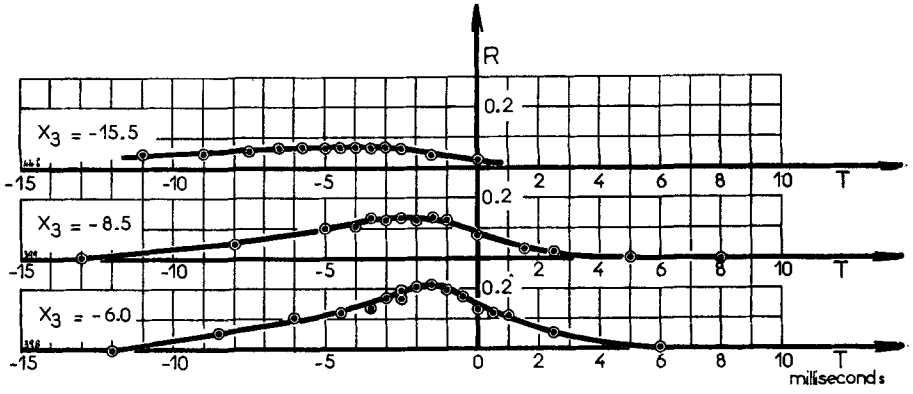

Figure 9. Transverse space-time correlations in the boundary layer on a flat plate downstream of a grid. ($y' = 1$ mm, $z = 79$ cm, $\delta = 16{\cdot}8$ mm).

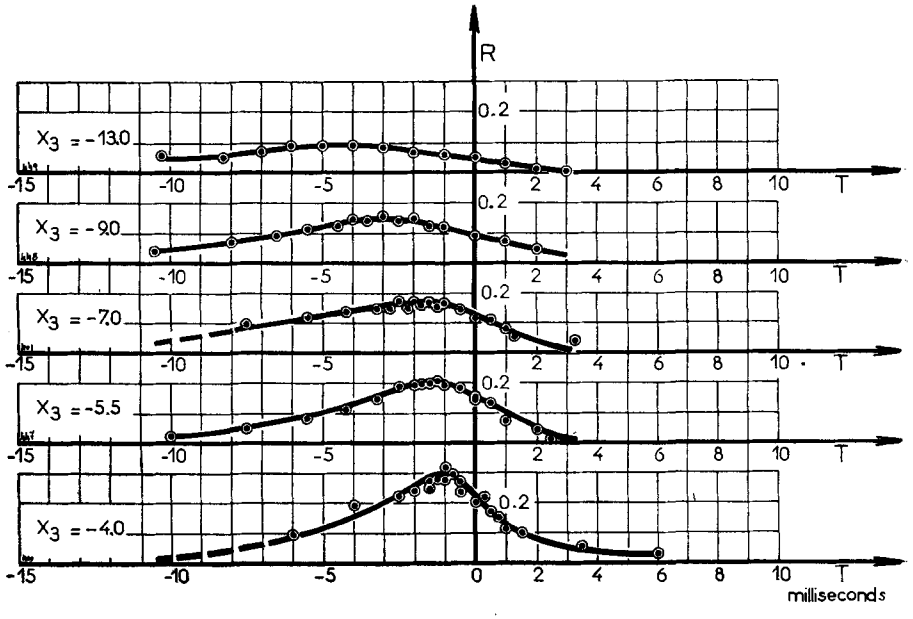

Figure 10. Transverse space-time correlations in the boundary layer on a flat plate downstream of a grid. ($y' = 1$ mm, $z = 74$ cm, $\delta = 16{\cdot}0$ mm).

One finds that the correlation reaches a maximum for a value T_i of the delay which is a function of X_3. Figure 13 summarizes the values of T_i. Note that for the distances from the leading edge $x = 74$ cm and $x = 79$ cm, which differ only by 3δ, the values of T_i are very little different. Note also that T_i changes sign with $X_3 = y' - y$.

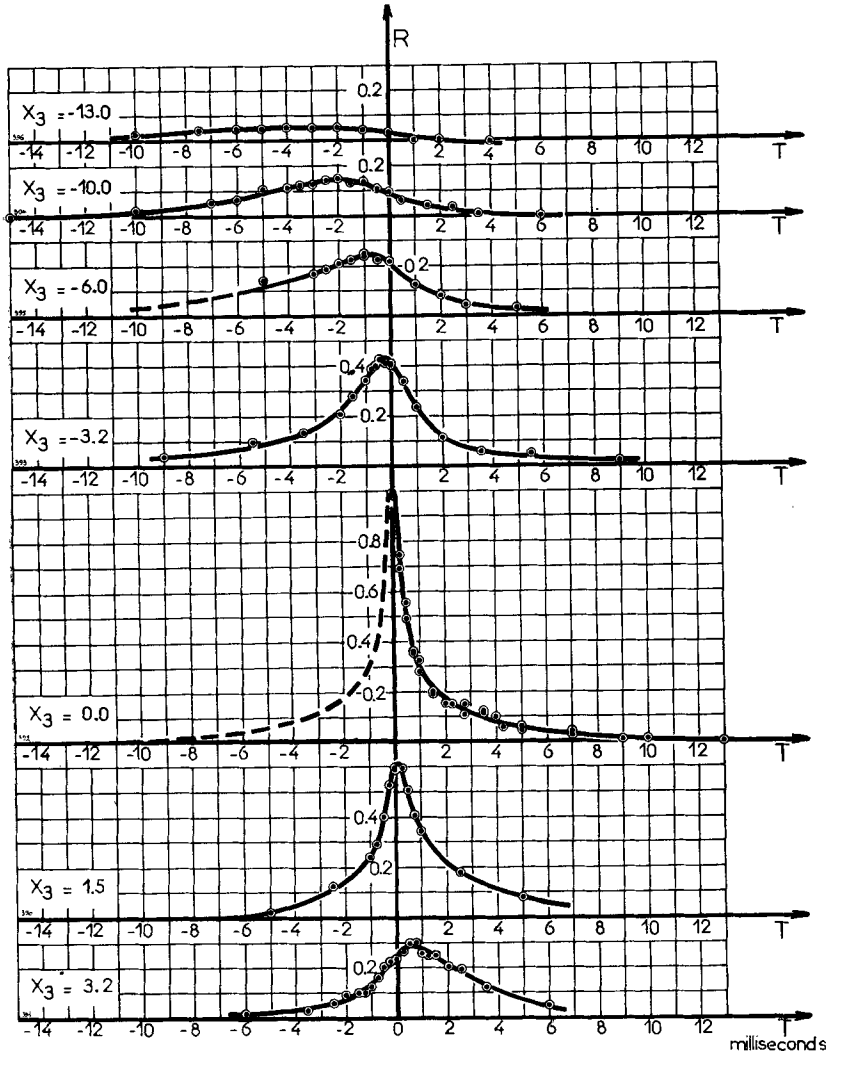

Figure 11. Transverse space-time correlations in the boundary layer on a flat plate downstream of a grid. ($y' = 4$ mm, $x = 79$ cm, $\delta = 16{\cdot}8$ mm).

In the case of the transition by roughness, the measurements have been made at two different stations, at distances $x = 79$ cm and $x = 194$ cm from the leading edge. The measurements of $R_{11}(T, X_1 = 0, X_2 = 0, X_3)$ at

the distance $z = 79$ cm are represented in figures 14 to 16, for which the data are:

figure 14, $y'/\delta = 0{\cdot}06$, $y' = 1$ mm;
figure 15, $y'/\delta = 0{\cdot}23$, $y' = 4$ mm;
figure 16, $y'/\delta = 0{\cdot}69$, $y' = 12$ mm.

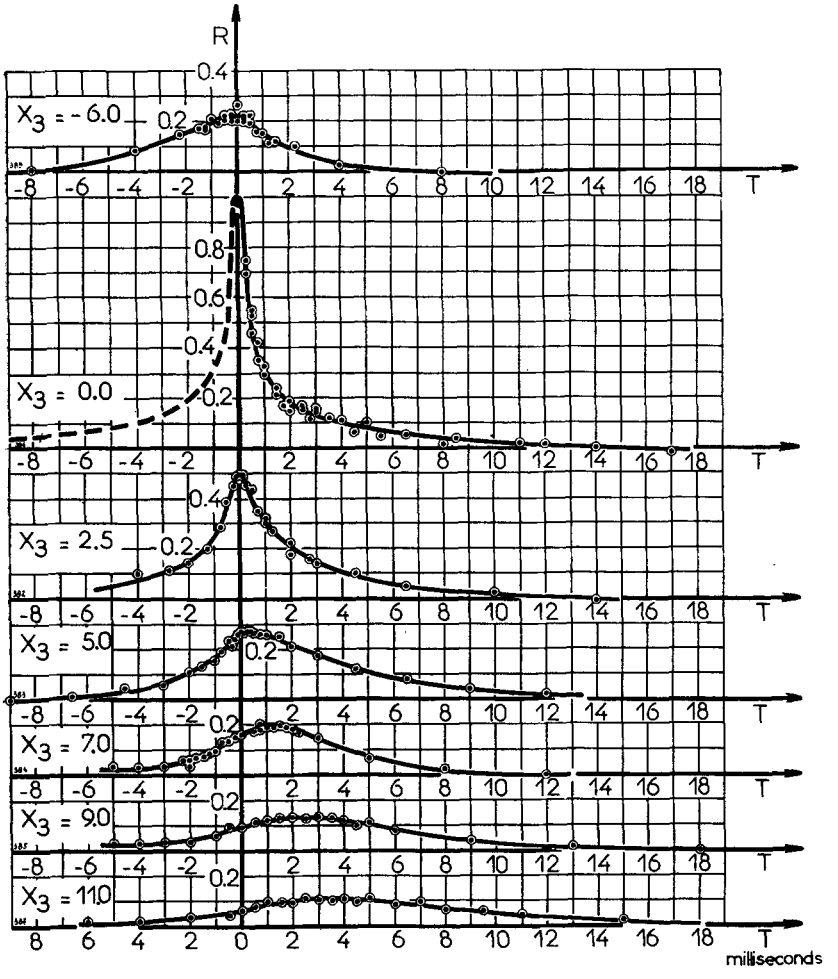

Figure 12. Transverse space-time correlations in the boundary layer on a flat plate, downstream of a grid. ($y' = 12$ mm, $z = 79$ cm, $\delta = 16{\cdot}8$ mm).

The measurements at the distance $z = 194$ cm are represented in figures 17 to 19, for which the data are:

figure 17, $y'/\delta = 0{\cdot}06$, $y' = 2$ mm;
figure 18, $y'/\delta = 0{\cdot}23$, $y' = 8$ mm;
figure 19, $y'/\delta = 0{\cdot}69$, $y' = 24$ mm.

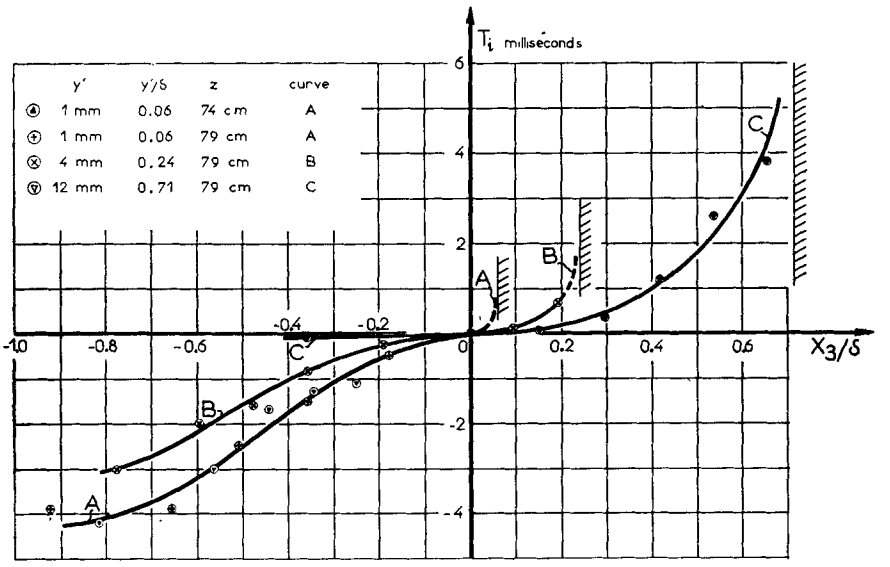

Figure 13. Optimum delays $T = T_i$ for transverse space-time correlations in the boundary layer on a flat plate downstream of a grid.

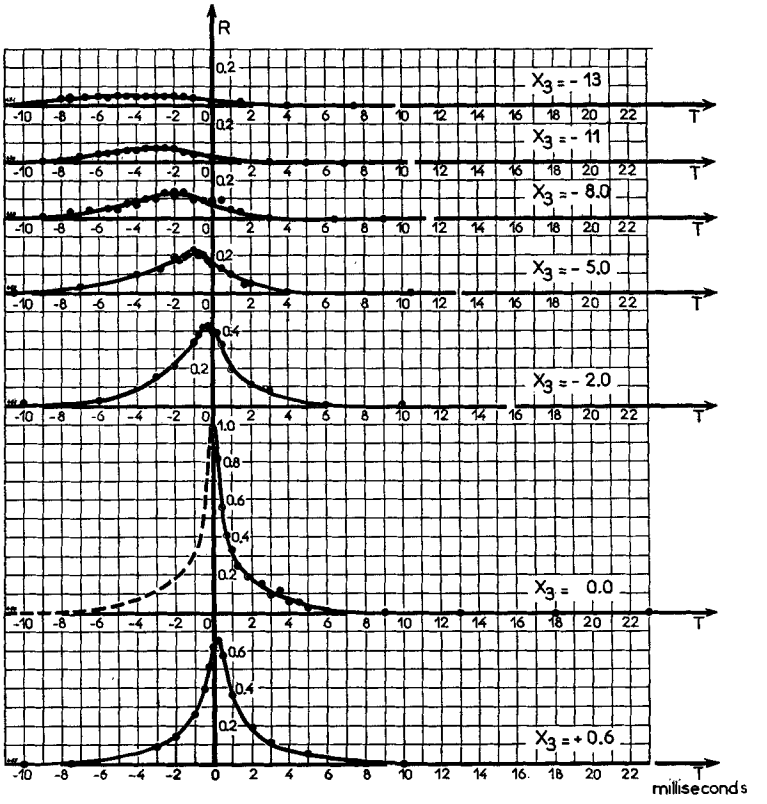

Figure 14. Transverse space-time correlations in the boundary layer on a flat plate with rough leading edge ($y' = 1$ mm, $z = 79$ cm, $\delta = 17{\cdot}5$ mm).

As in the case of transition by preturbulence, one finds that the correlation reaches a maximum for a value T_i of the delay which is a function of X_3. Figure 20 summarizes the values of T_i which change sign with X_3.

The values of T_i obtained at the distances $z = 74$ cm and $z = 79$ cm from the leading edge and for a thickness of the boundary layer of the same order are only slightly different, whether the transition is due to preturbulence (figure 13) or roughness (figure 20). Also, the curves for the distribution of the corresponding mean velocities are also only slightly different.

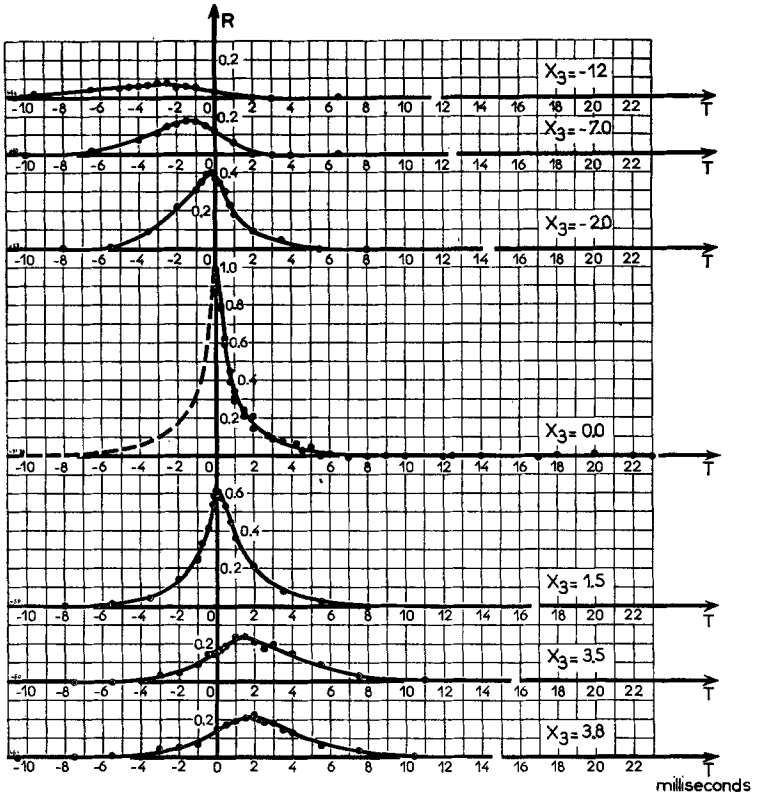

Figure 15. Transverse space-time correlations in the boundary layer on a flat plate with rough leading edge ($y' = 4$ mm, $z = 79$ cm, $\delta = 17{\cdot}5$ mm).

The measurements of T_i made at the two distances $z = 79$ cm and $z = 194$ cm (distances which differ by about 45 times the average thickness of the boundary layer) show that, X_3 being fixed, the delay T_i generally increases with the distance z from the leading edge, in the direction of increasing thickness of the boundary layer. Moreover, this increase of T_i is much smaller than the differences of the delays τ_y corresponding to the transport due to the mean motion, if one considers this transport over the distance separating the position $z = 79$ cm from the position $\dot{z} = 194$ cm (this delay, along the isochronous lines is $\tau_{y'} - \tau_y = (\dot{z} - z)(1/V' - 1/V)$).

y'/δ	y/δ	$\lvert\tau_{y'}-\tau_y\rvert$ (ms)	$\lvert(T_i)_z-(T_i)_z\rvert$ (ms)	$\dfrac{\lvert\tau_{y'}-\tau_y\rvert}{\lvert(T_i)_z-(T_i)_z\rvert}$
0·06	0·76	68	3·2	21
	0·46	56	2·2	25
	0·26	43	1·3	33
0·23	0·63	23	1·3	18
	0·43	13·5	0·6	32
	0·13	9·4	0·3	31
	0·03	54	0·05	1000
0·69	0·49	8·5	0·45	19
	0·29	22	1·25	18
	0·09	47	1·6	29

Table 1.

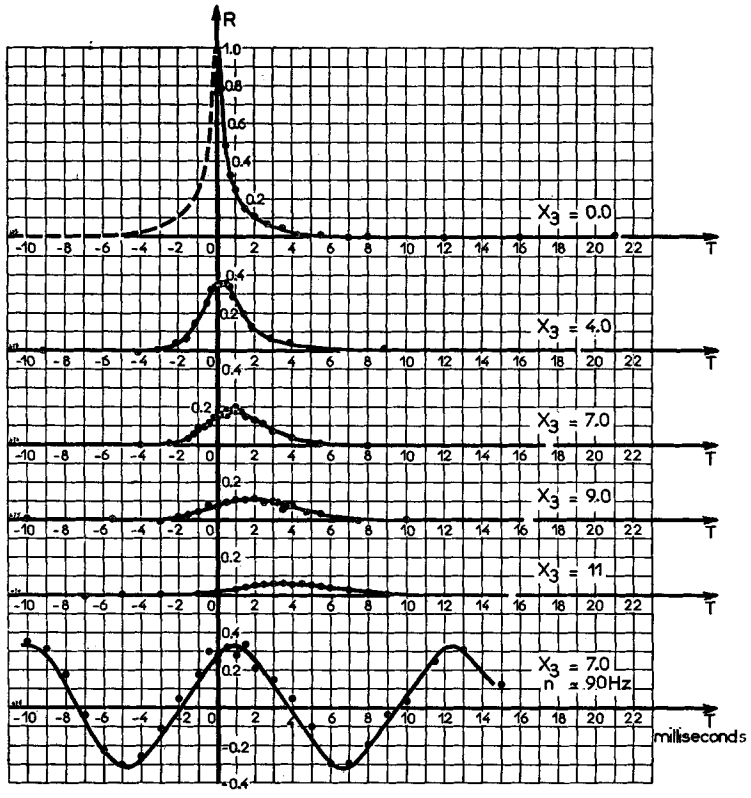

Figure 16. Transverse space-time correlations in the boundary layer on a flat plate with rough leading edge ($y' = 12$ mm, $z = 79$ cm, $\delta = 17{\cdot}5$ mm).

Table 1 gives this comparison, in the case of the distances z mentioned above.

Measurements of $R_{11}(T, X_1 = 0, X_2 = 0, X_3)$ have also been made by means of a double analyser which admitted only the waves of frequencies of about 90 hertz. When $z = 79$ cm, $y'/\delta = 0{\cdot}69$, $X_3/\delta = 0{\cdot}40$ ($nF(\epsilon) \doteqdot 0{\cdot}32$), we see from figure 16 that the maximum correlation 0·33 is reached for a delay T_i of about 0·95 ms. When $z = 194$ cm, $y'/\delta = 0{\cdot}71$, $X_3/\delta = 0{\cdot}38$ ($nF(\epsilon) \doteqdot 0{\cdot}60$), figure 19 shows that the maximum correlation 0·22 is reached for a delay T_i of about 2·2 ms. So, in both cases, the value of T_i is not practically modified, and that of the correlation is increased by filtering, but this is not very significant because these frequencies are in the middle of the spectrum.

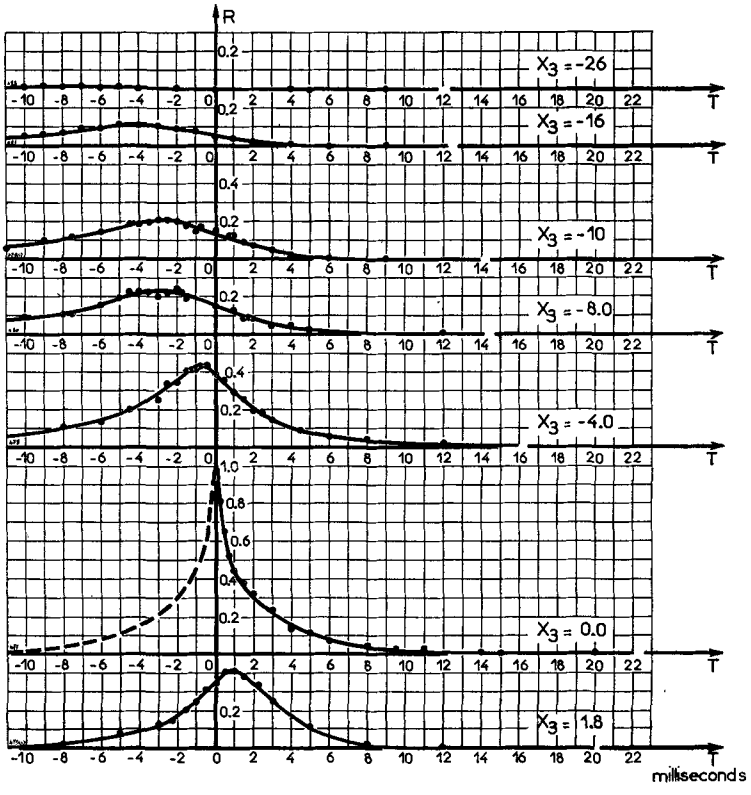

Figure 17. Transverse space-time correlations in the boundary layer on a flat plate with rough leading edge ($y' = 2$ mm, $z = 194$ cm, $\delta = 34$ mm).

We turn now to the longitudinal space-time correlations $R_{11}(T, X_1, X_2 = 0, X_3 = 0)$. Let us recall that we tried (Favre, Gaviglio & Dumas 1953 b) to obtain a verification of Taylor's hypothesis for the turbulence downstream of a grid, and found a satisfactory concordance of the autocorrelation curves with the curves of longitudinal space correlation, established up to a distance X_1/M of about 8, with the

correspondence $T = X_1/V$; but for distances $X_1/M > 1{\cdot}5$, the correlations being smaller than 0·1, the comparison is no longer conclusive.

Further verification, including measurements of the longitudinal space-time correlations (up to $X_1/M = 8$) with optimum delay to compensate for the transport due to the mean flow, has shown that these correlations retain high values, of the order of 0·5, up to great distances $X_1/M = 5$ to 8, these values not being, however, equal to unity.

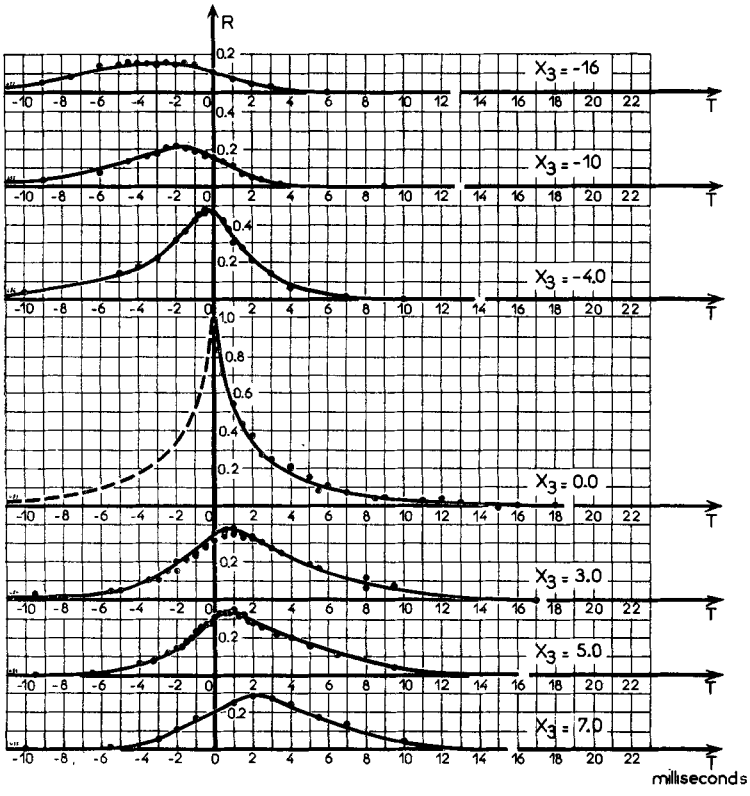

Figure 18. Transverse space-time correlations in the boundary layer on a flat plate with rough leading edge ($y' = 8$ mm, $x = 194$ cm, $\delta = 34$ mm).

In the conditions of the present experiments relating to the boundary layer, with transition by preturbulence, we have attempted a similar comparison, with a view to a possible extension of Taylor's hypothesis.

Figure 21 presents, for $y'/\delta = 0{\cdot}24$, the comparison of the two auto-correlation curves $R_{11}(T, X_1 = X_2 = X_3 = 0)$ (at positions $x = 74$ cm and $x = 79$ cm) with the longitudinal correlation curve $R_{11}(T = 0, X_1, X_2 = X_3 = 0)$ obtained along a line $X_3 = 0$, which here is not very different from the streamline. In this case there is still a satisfactory concordance between

the autocorrelation and the longitudinal space correlation, established up to X_1/M of about 2·5 (i.e. $X_1/V = 5{\cdot}2$ ms), but for $X_1/M \geqslant 2$ (or $X_1/V \geqslant 4$ ms), the correlations being smaller than 0·1, the comparison is no longer conclusive.

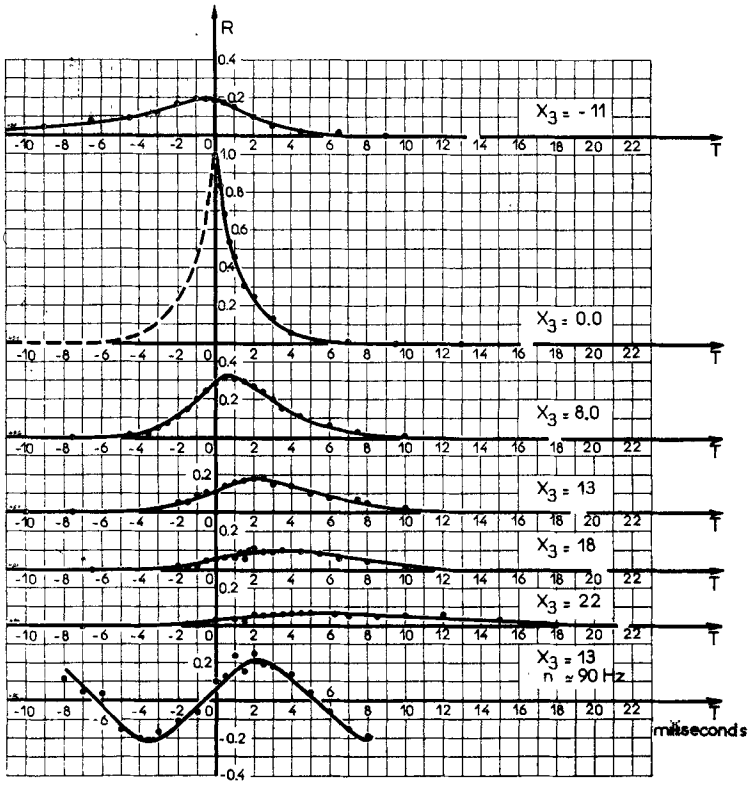

Figure 19. Transverse space-time correlations in the boundary layer on a flat plate with rough leading edge ($y' = 24$ mm, $x = 194$ cm, $\delta = 34$ mm).

y'/δ	1	0·71	0·24	0·06
$(X_1/M)_{R=0{\cdot}5}$	5 to 8	5·0	1·6	0·8
$(X_1/\delta)_{R=0{\cdot}5}$	7·5 to 12	7·5	2·4	1·2

Table 2.

Further verification, including the measurement of the longitudinal and transverse space-time correlations $R_{11}(T, X_1, X_2 = 0, X_3)$ along the line of maximum correlation, with an optimum delay $T = T_m$ (see below), shows (figure 30) that this correlation retains high values of the order of 0·5 up to the distances $(X_1/\delta)_{R=0{\cdot}5}$ or $(X_1/M)_{R=0{\cdot}5}$ given in table 2, but these distances decrease rapidly with the distance y'/δ of the upstream wire from the wall.

Measurements of the longitudinal and transverse space-time correlations $R_{11}(T, X_1, X_2 = 0, X_3)$ have been made in the case of the transition by preturbulence, using the old type of probes. The upstream hot wire A was fixed, at a distance $x = 74$ cm from the leading edge, and at a distance y' from the wall. The hot wire B was placed at the distance X_1 downstream

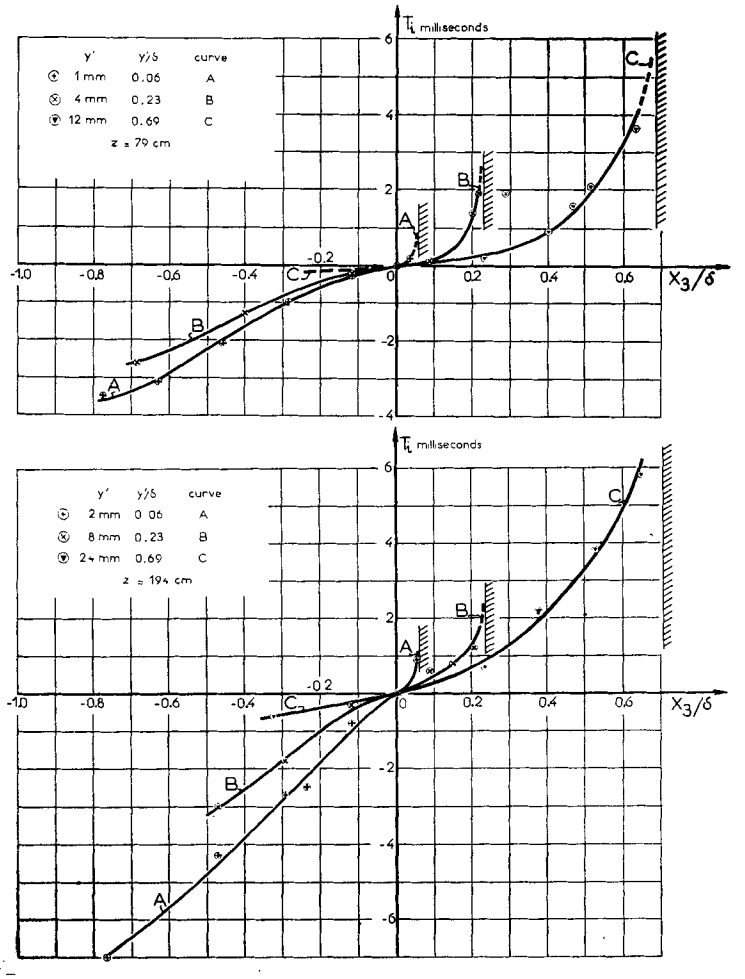

Figure 20. Optimum delays $T = T_i$ for transverse space-time correlations in the boundary layer on a flat plate with rough leading edge.

of A. Its distance y to the wall and consequently X_3, was varied. The delay T was also varied. The results are presented in figures 22 to 25, which correspond to the following conditions:

figure 22, $y'/\delta = 0{\cdot}06$, $y' = 1$ mm, $X_1 = 25{\cdot}4$ mm;
figure 23, $y'/\delta = 0{\cdot}06$, $y' = 1$ mm, $X_1 = 50{\cdot}8$ mm;
figure 24, $y'/\delta = 0{\cdot}24$, $y' = 4$ mm, $X_1 = 25{\cdot}4$ mm;
figure 25, $y'/\delta = 0{\cdot}24$, $y' = 4$ mm, $X_1 = 50{\cdot}8$ mm.

They follow the results published (Favre, Gaviglio & Dumas 1954b) for the conditions $y'/\delta = 0{\cdot}71$, $y' = 13$ mm, $X_1 = 49$ mm. The correlation is found to reach a maximum for an optimum value T_m of the delay, which is a function of X_3.

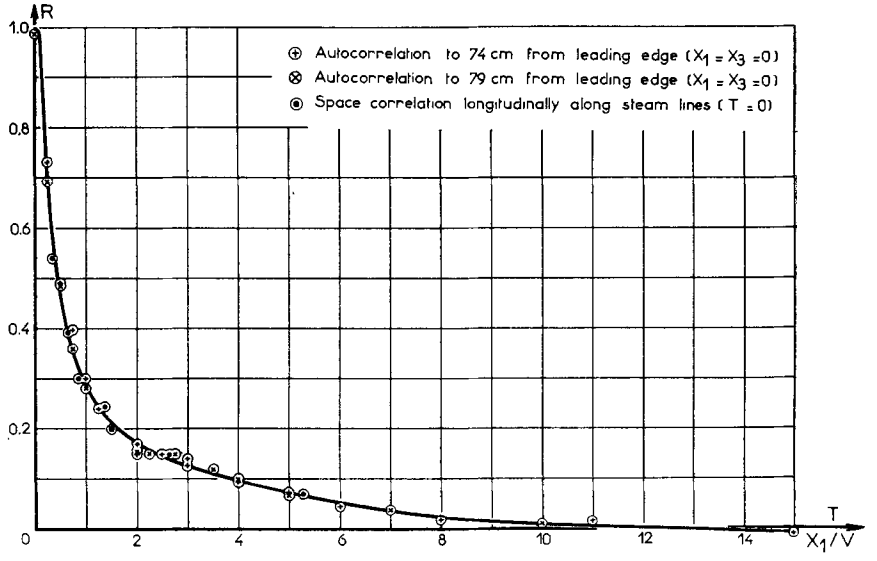

Figure 21. Check on Taylor's hypothesis for the boundary layer on a flat plate downstream of a grid ($y' = 4$ mm, $y/\delta = 0{\cdot}24$).

Figure 26 gives the values of T_m and their comparison with the computed values. The computation is made as previously (Favre, Gaviglio & Dumas 1954b), that is, by assuming (as a first approximation in the case of these experiments) that *the optimum delays T_m differ from the delays T_i by time intervals which are equal to the delays T_c compensating for the transport due to the mean flow** ;

$$T_m \sim T_i + T_c.$$

This relation is still satisfactory when, the upstream wire being at a distance from the wall $y'/\delta = 0{\cdot}24$, the downstream wire itself is at a distance $y/\delta \geqslant 0{\cdot}04$; also when $y'/\delta = 0{\cdot}06$ for $y/\delta \geqslant 0{\cdot}09$. For shorter distances, the relation is less satisfactory, either on account of the disturbances brought about by the probe or because supplementary terms should be introduced.

Figures 27 and 28 indicate that, as we have shown elsewhere (Favre, Gaviglio & Dumas 1954b), the introduction of the optimum delay T_m increases the correlation in a large proportion (of the order of 2·55 to 5·5 in the cases examined). The *maximum maximorum* of the space-time correlations, $R_{\max}(T = T_m, X_1, X_2 = 0, X_3)$, corresponding to given X_1, is

* T_c is given, to a sufficient approximation, by $T_c = 2X_1/(V_A + V_B)$.

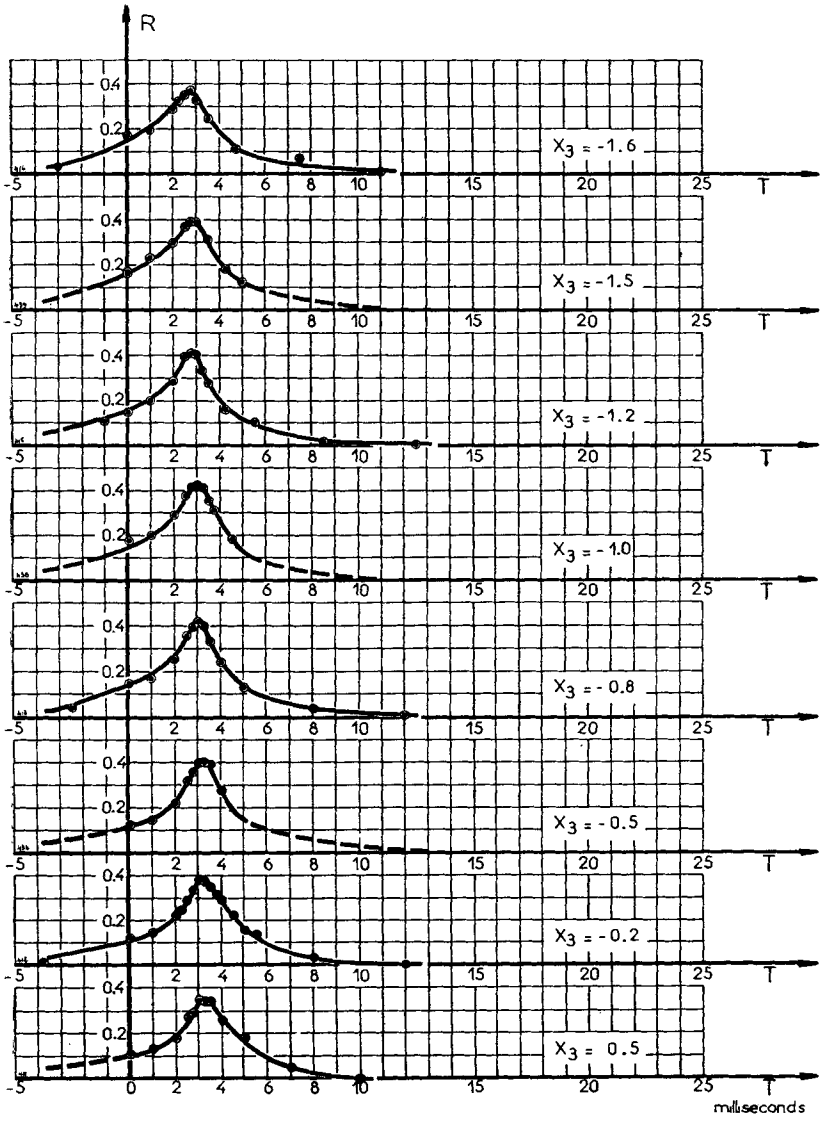

Figure 22. Transverse and longitudinal space-time correlations in the boundary layer on a flat plate downstream of a grid ($y' = 1$ mm, $y'/\delta = 0{\cdot}06$, $X_1 = 25{\cdot}4$ mm).

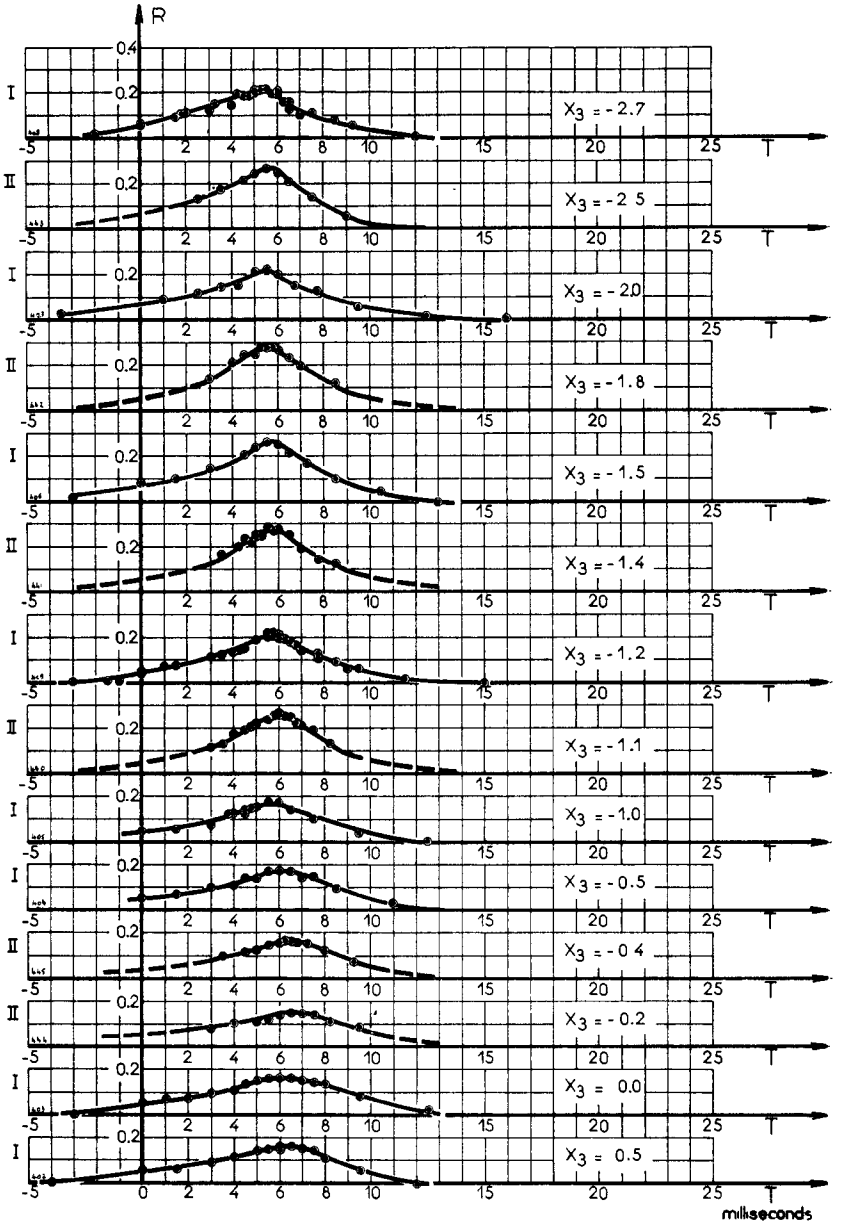

Figure 23. Transverse and longitudinal space-time correlations in the boundary layer on a flat plate downstream of a grid ($y' = 1$ mm, $y'/\delta = 0{\cdot}06$, $X_1 = 50{\cdot}8$ mm). I. First series of measurements. II. Second series of measurements.

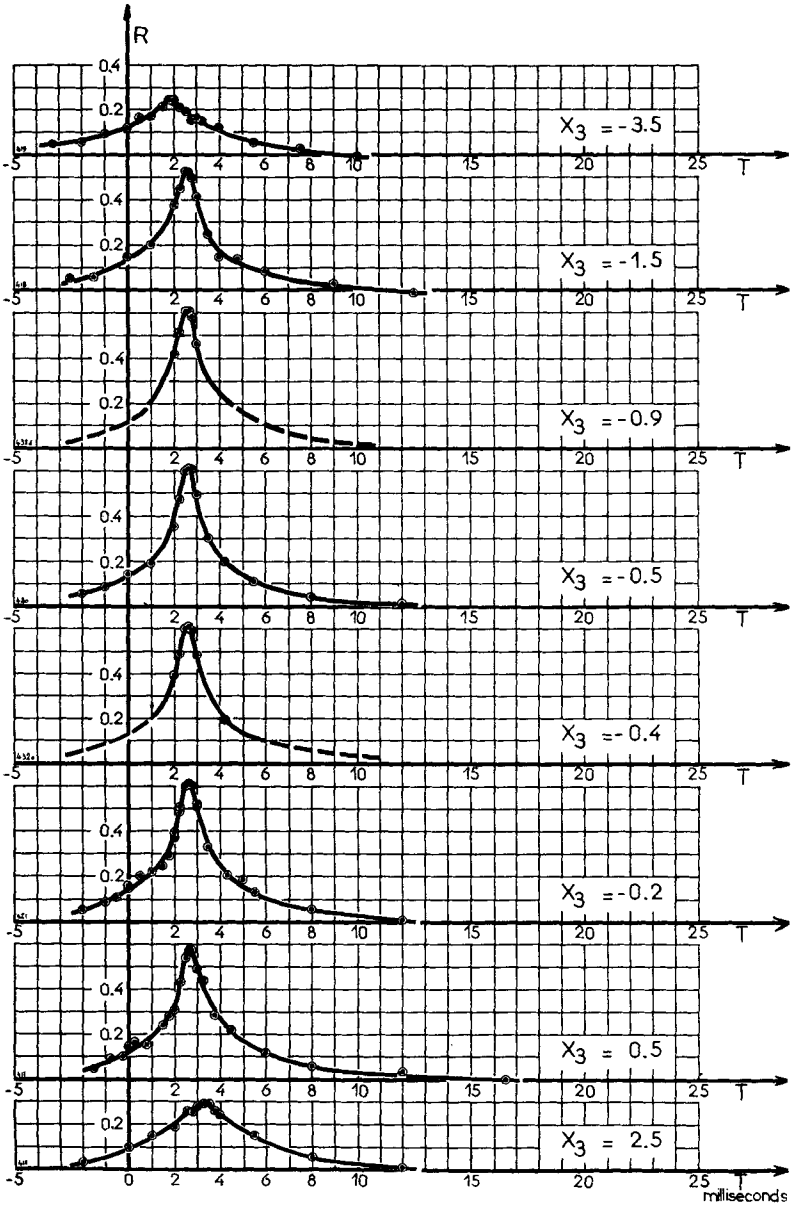

Figure 24. Transverse and longitudinal space-time correlations in the boundary layer on a flat plate downstream of a grid ($y' = 4$ mm, $y'/\delta = 0{\cdot}24$, $X_1 = 25{\cdot}4$ mm).

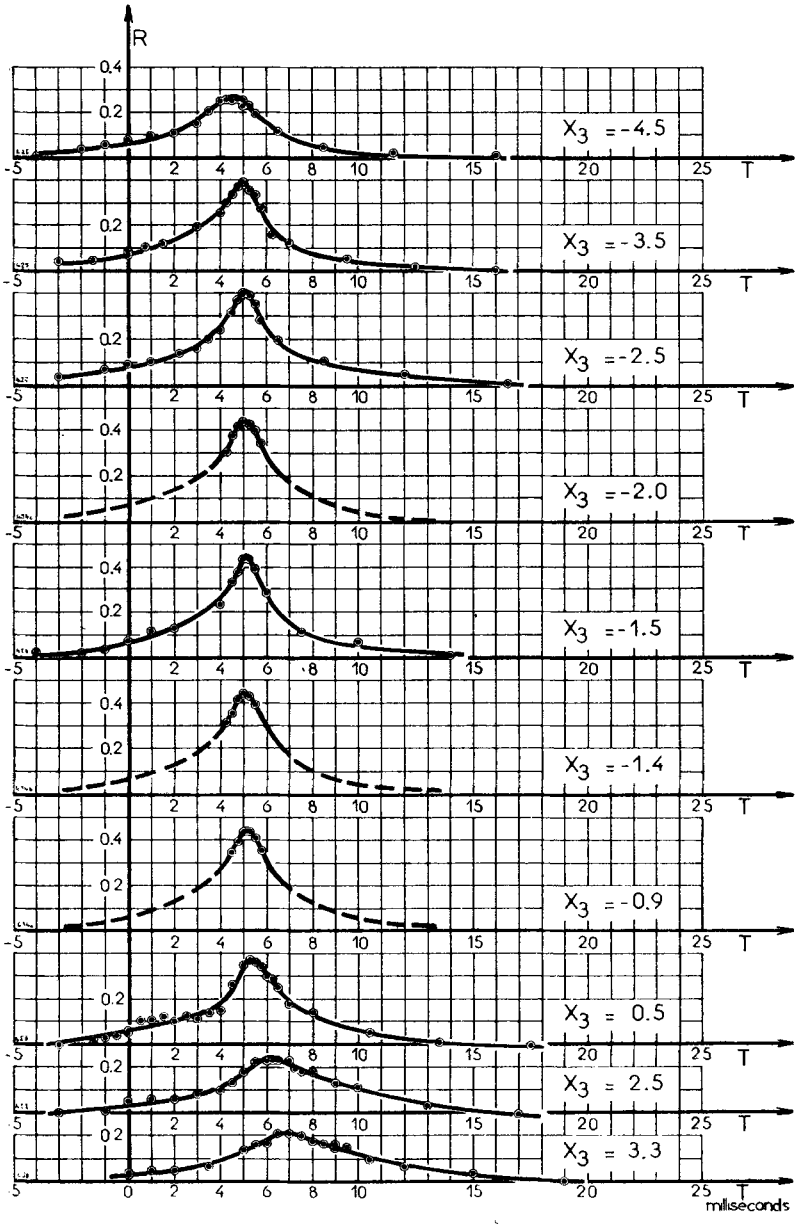

Figure 25. Transverse and longitudinal space-time correlations in the boundary layer on a flat plate downstream of a grid ($y' = 4$ mm, $y'/\delta = 0{\cdot}24$, $X_1 = 50{\cdot}8$ mm).

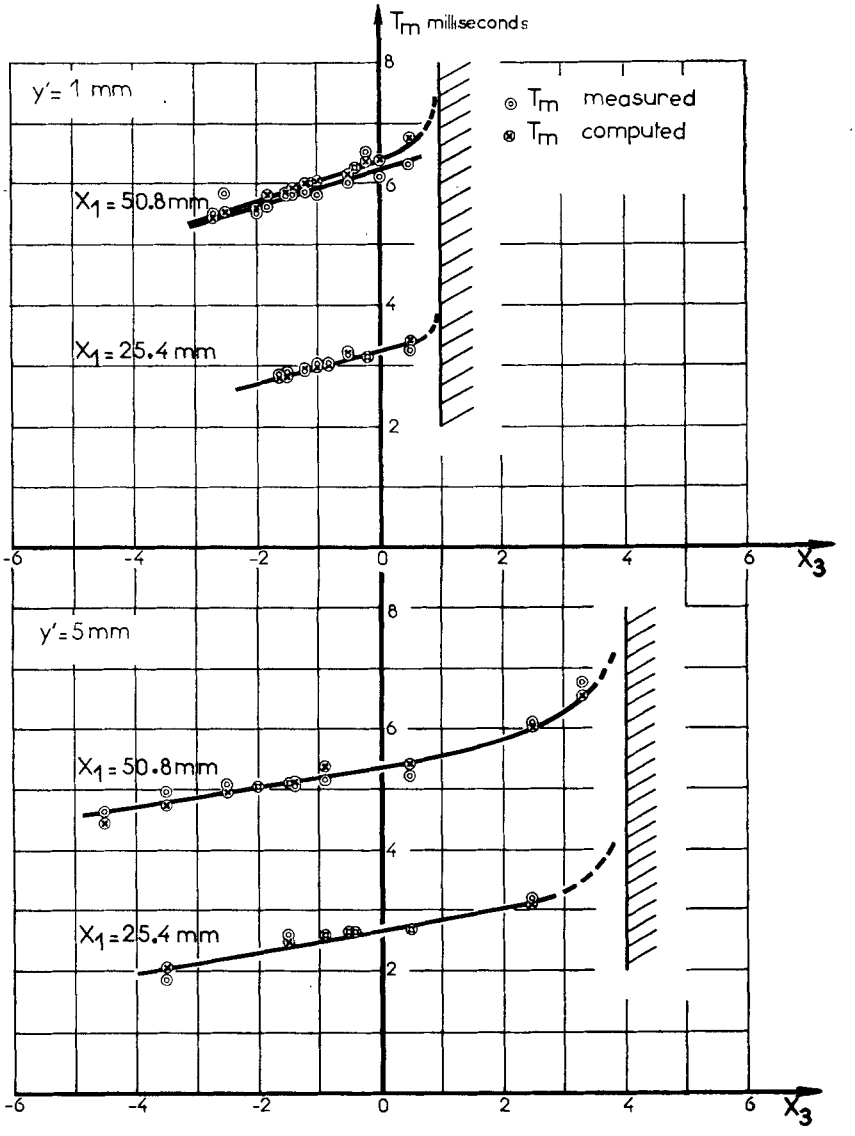

Figure 26. Optimum delays $T = T_m$ for transverse and longitudinal correlations. Transition by preturbulence.

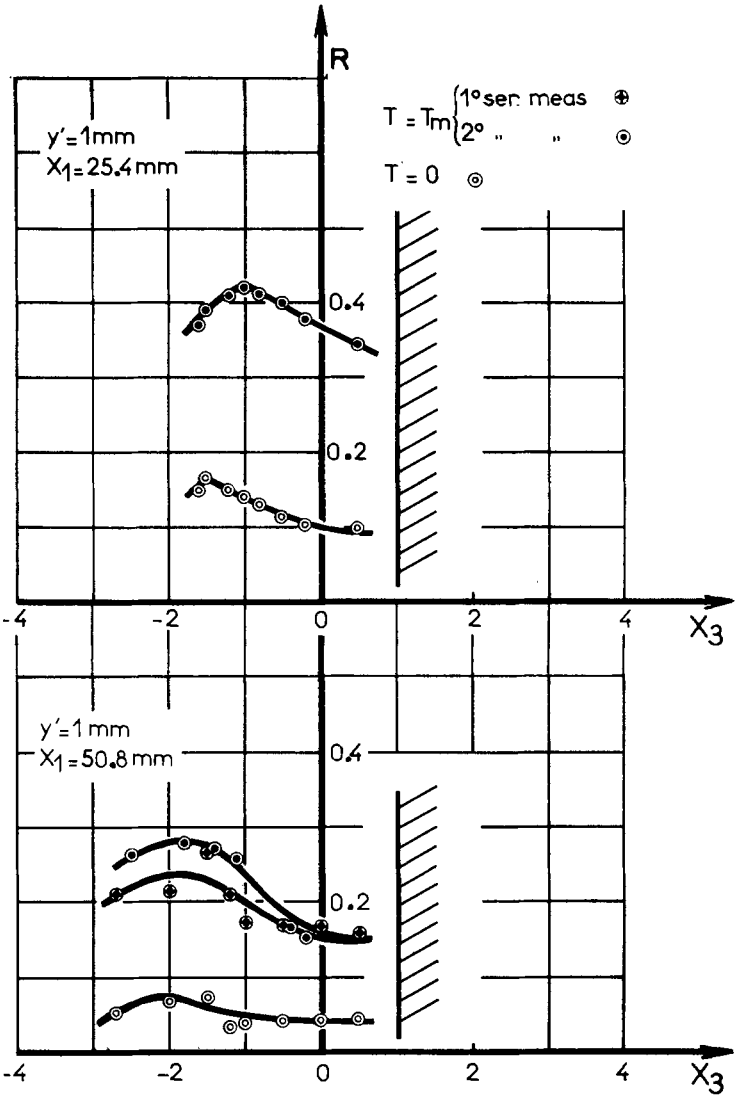

Figure 27. Comparison between transverse and longitudinal correlations with zero-delay ($T = 0$) and transverse and longitudinal correlations with optimum delay ($T = T_m$). Transition by preturbulence ($x = 74$ cm).

obtained for a certain value of X_3. Likewise the maximum of the space-time correlations, $R_{\max}(T = 0, X_1, X_2 = 0, X_3)$, corresponding to given X_1, is obtained for $T = 0$ and for a certain value of X_3, different from the previous one. In figure 29 have been drawn the lines of maximum space-time

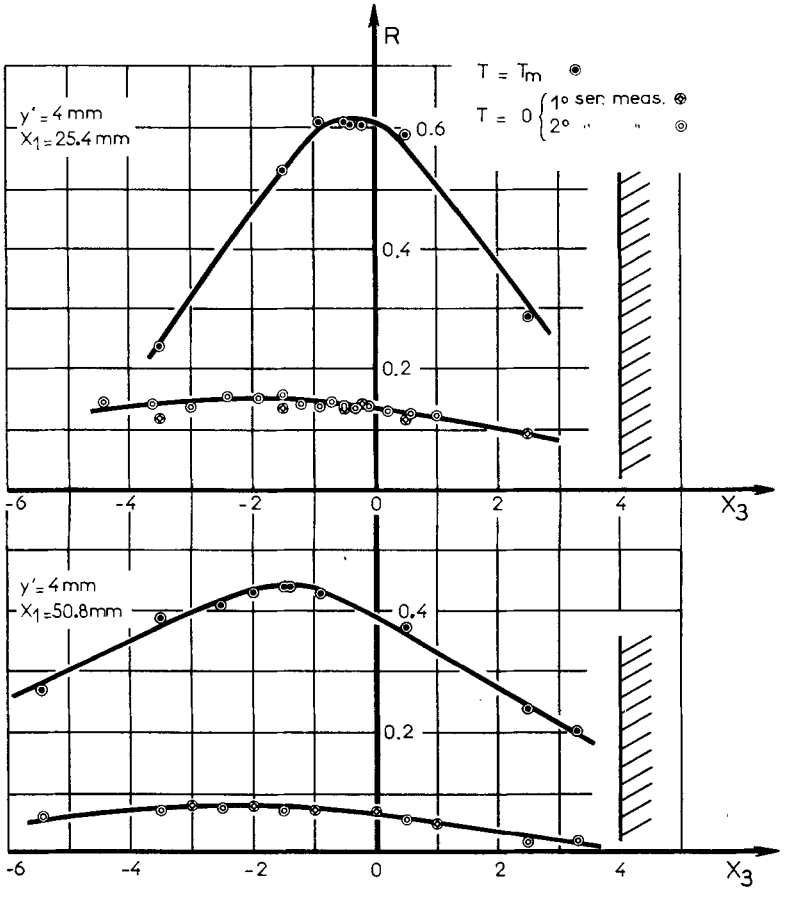

Figure 28. Comparison between transverse and longitudinal space-time correlations with zero delay ($T = 0$) and transverse and longitudinal space-time correlations with optimum delays ($T = T_m$). Transition by preturbulence ($x = 74$ cm.).

correlations with optimum delay ($T = T_m$), and also the lines of maximum correlations with zero delay ($T = 0$). Outside the boundary layer, these lines coincide with the mean streamlines (Favre, Gaviglio & Dumas 1953 b), but inside the boundary layer, they are markedly different from the streamlines. Table 3 summarizes the results.

Figure 30 shows the space-time correlations outside the boundary layer ($y'/\delta \geqslant 1$) and inside the boundary layer ($y'/\delta = 0{\cdot}71$, $0{\cdot}24$, $0{\cdot}06$), along the line of maximum space-time correlations, relative to the upstream wire position. $S_{y'}$ and S_y represent the curvilinear abscissae of the upstream

y'/δ	X_1	X_3	$R_{11\max}$ $(T = T_m, X_1, X_2 = 0, X_3)$	$R_{11\max}$ $(T = 0, X_1, X_2 = 0, X_3)$
0·06	25·4	−1	0·42	
		−1·6		0·165
	50·8	−1·8	0·28 or 0·24	
		−2·0		0·070
0·24	25·4	−0·5	0·62	
		−1·6		0·160
	50·8	−1·5	0·44	
		−2·2		0·080
0·71	49·0	−1·3	0·705	
		−2·8		0·160

Table 3.

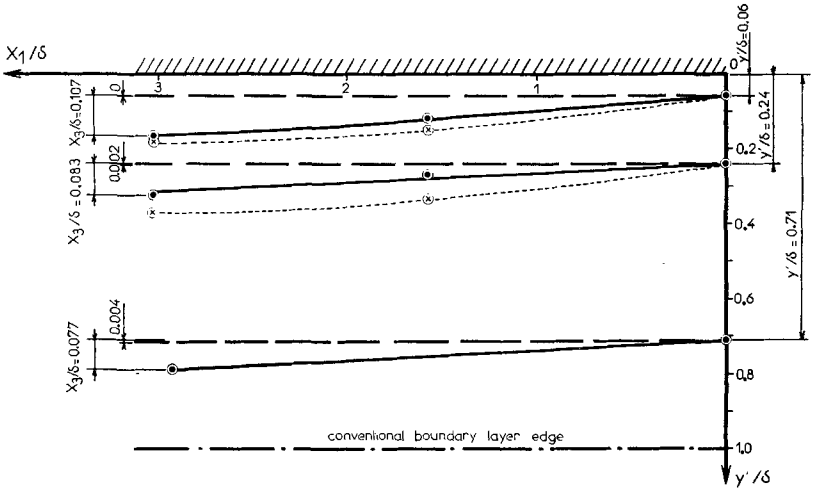

Figure 29. Lines of maximum correlation with optimum delay ($T = T_m$) —⊙— Lines of maximum correlation with zero delay ($T = 0$) - - - - -⊗- - - - - Stream-lines ——— ——— ——— (downstream of a grid).

and downstream wires along this line. When $T = T_m$ one gets the curves of space-time correlation along the line of maximum space-time correlation, with optimum delay. As we have noted above these curves show that the correlation retains high values of the order of 0·5 up to distances $(X_1/\delta)_{R\,=\,0{\cdot}5}$ which decrease rapidly with the distance y'/δ of the upstream wire from the wall.

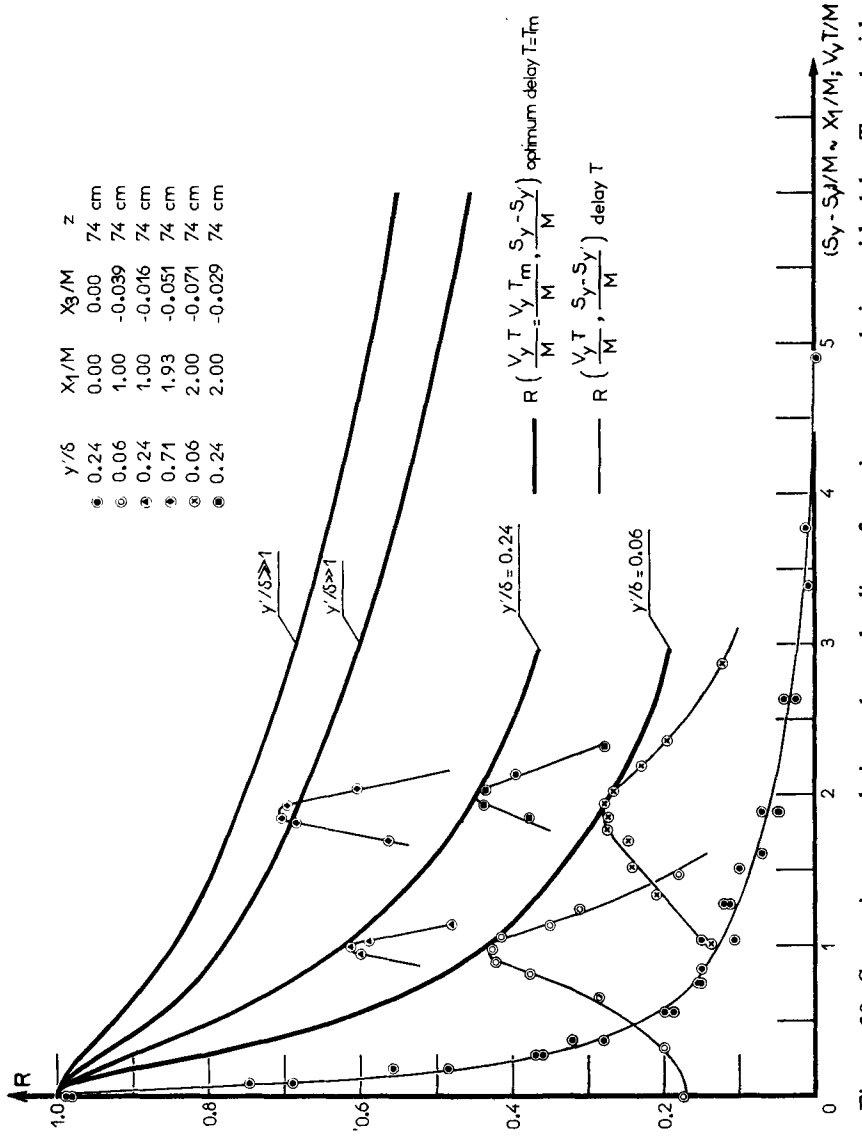

Figure 30. Space-time correlations along the line of maximum correlation with delay T, and with optimum delay $T = T_m$, in the boundary layer on a flat plate downstream of a grid,

In figure 31 are reproduced the space-time isocorrelation curves with optimum delay $T = T_m$, for the distances to the wall of the upstream wire $y'/\delta = 0{\cdot}06$, $0{\cdot}24$ and $0{\cdot}71$.

Measurements are being continued, with improved accuracy.

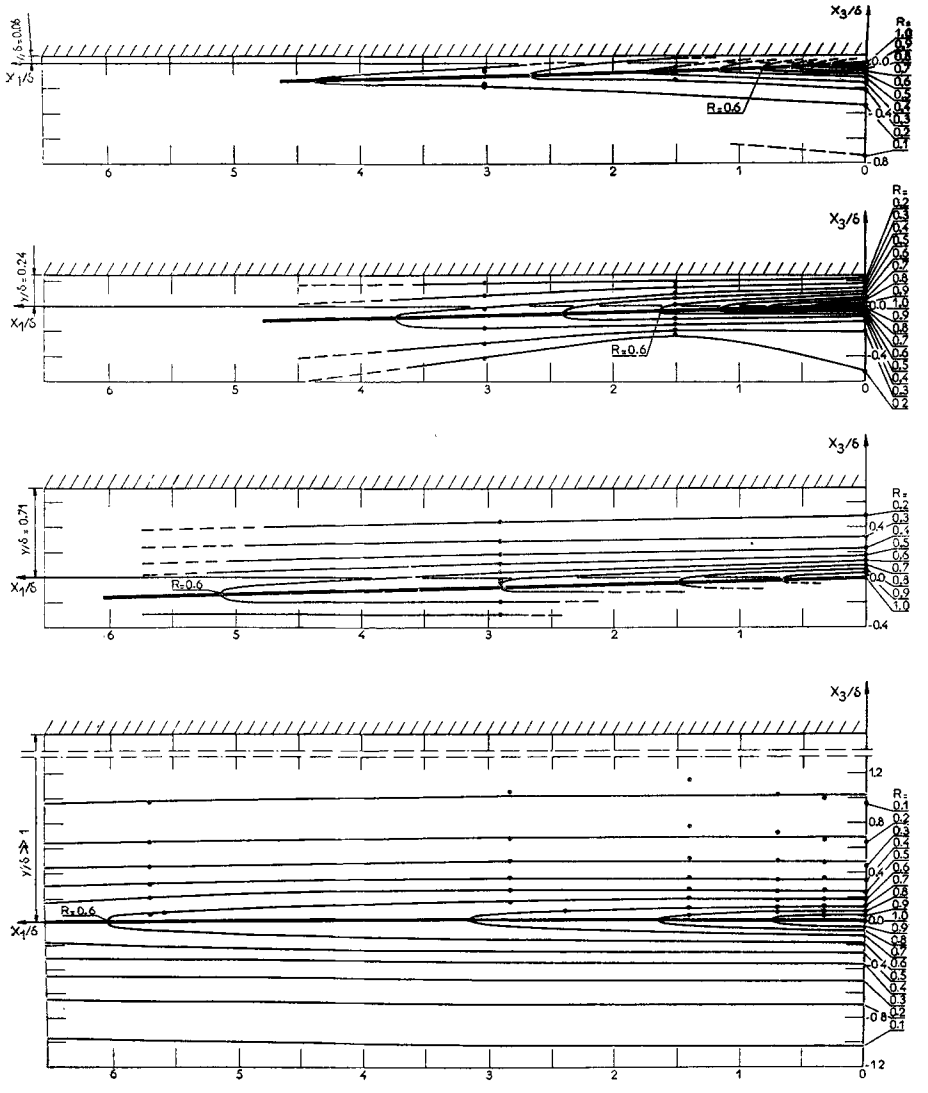

Figure 31. Space-time isocorrelation with optimum delay, in the boundary layer on a flat downstream of a grid.

These researches were made at the Laboratoire de Mécanique de l'Atmosphère (I.M.F. Marseille) for the Office National d'Etudes et de Recherches Aéronautiques (O.N.E.R.A.) with the aid of the Ministère de l'Air and of the Centre National de la Recherche Scientifique.

References

Clauser, F. H. 1954 *J. Aero. Sci.* **21**, 91.

Corrsin, S. & Kistler, A. L. 1954 *Nat. Adv. Comm. Aero., Wash., Tech. Note* no. 3133.

Favre, A. 1946 *Proc. 6th Inter. Congr. Appl. Mech.*

Favre, A. 1948 *Proc. 7th Inter. Congr. Appl. Mech.*

Favre, A., Gaviglio, J. & Dumas, R. 1952 *Publ. Sci. Tech. Minist. de l'Air*, no. 296.

Favre, A., Gaviglio, J. & Dumas, R. 1953 a *La Rech. Aéro.*, no. 31.

Favre, A., Gaviglio, J. & Dumas, R. 1953 b *La Rech. Aéro.*, no. 32.

Favre, A., Gaviglio, J. & Dumas, R. 1954 a *La Rech. Aéro.*, no. 38.

Favre, A., Gaviglio, J. & Dumas, R. 1954 b *La Rech. Aéro.*, no. 39.

Favre, A., Gaviglio, J. & Dumas, R. 1955 *La Rech. Aéro.* no. 48.

Klebanoff, P. S. & Diehl, Z. W. 1952 *Nat. Adv. Comm. Aero., Wash., Rep.* no. 1110.

Liepmann, H. W. 1952 *Z. angew. Math. Phys.* **3**, 321 and 407.

Phillips, O. M. 1954 *Proc. Camb. Phil. Soc.* **51**, 220.

Squire, H. B., Winter, K. G. & Barnes, E. G. 1947 *Royal Aircraft Establishment, Rep. Aero.* no. 2182.

Taylor, G. I. 1948 *Proc. Roy. Soc.* A, **164**, 476.